Dielectric control of spin in semiconductor spherical quantum dots

J. Planelles,[a] F. Rajadell, and M. Royo
Departament de Química Física i Analítica, UJI, Box 224, E-12080 Castelló, Spain

(Received 9 April 2008; accepted 1 May 2008; published online 14 July 2008)

The ground state electronic configuration of semiconductor spherical quantum dots populated with different numbers of excess electrons, for different radii and dielectric constants of the embedding medium is calculated and the corresponding phase diagram drawn. To this end, an extension of the spin density functional theory to study systems with variable effective mass and dielectric constant is employed. Our results show that high/low spin configurations can be switched by appropriate changes in the quantum dot embedding environment and suggest the use of the quantum dot spin as a sensor of the dielectric response of media. © *2008 American Institute of Physics*.
[DOI: 10.1063/1.2952070]

I. INTRODUCTION

Control over single, localized spins has long been recognized as a relevant issue in fabricated nanostructures and devices.[1] The new building blocks for such devices are quantum dots (QDs), i.e., semiconductor nanostructures that confine carriers in all three spatial dimensions. A very precise fabrication process allows the strength of the QD confinement to be tailored while a gate voltage can tune its countable number of electrons.[2] The great flexibility in designing QDs with precise properties has attracted a large amount of research both in science and technology in the last decade,[3] leading QDs to be employed in many technological applications such as optical switches,[4] light-emitting diodes,[5] photovoltaic cells,[6] etc. Recently, colloidal spherical quantum dots have also proven to offer high performance in biological and medical applications.[7] A specific characteristic of biological and, in general, organic environments is their huge dielectric mismatch with typical inorganic semiconductor QD structures. When QDs are embedded in such environments, the formation of polarization charges at the interface may strongly influence confinement and modify the distribution of charge carriers inside the QD. The effects of dielectric mismatches therefore cannot be overlooked in the theoretical description.[8] Thus, enhancement of the electron-electron Coulomb interaction, which arises from polarization effects, is found to induce reconstructions of the electronic configurations as the dot is filled with carriers.[9–12]

There are various parameters that influence the electronic configuration in semiconductor quantum dots, such as the number of electrons, the shape and strength of the confining potential and external fields. The key ingredient for manipulating the way of spin filling is the tuning of orbital degeneracies. One can have, for example, a triplet state with two parallel spin electrons in two different but nearly degenerate orbitals. The excited state is then a spin singlet having the same orbital configuration but with antiparallel spins.

Manipulation of orbital degeneracies in quantum dots is usually carried out by magnetic fields in the relatively low range of magnetic field strengths. Among others, we may mention studies on triplet-singlet transitions induced by a magnetic field.[13] In the high magnetic field range the interaction effect becomes more important than the effect of quantum mechanical confinement because all the electrons are confined to the lowest Landau level. This gives rise to a fully spin-polarized state.

A remarkable many-particle phenomenon observed in a quantum dot, when tuning ground-state degeneracy between triplet- and singlet-spin states, is the so-called integer Kondo effect.[14] This effect is also predicted as coming from degeneracy tuned by disorder[15] and can occur for impurities and quantum dots that have a spin of 1, or higher.[16]

We focus our attention on the role of dielectric mismatch in QD spin transitions. We draw the ground state spin phase diagram of a semiconductor spherical quantum dot populated with different numbers of electrons versus the dielectric response of the embedding media. To this end, we work within the spin density functional theory (SDFT) framework. Particularly, we use a method we recently developed[11] and tested[11,12] that is capable of studying many-electron spherical QDs including effective mass and dielectric mismatches between the QD and the surrounding medium. Our results evidence the possibility of switching between high/low spin configurations by changing the QD embedding environment, and suggest the use of QD spin as a sensor of the dielectric response of a given medium.

II. THEORY AND COMPUTATIONAL DETAILS

Calculations are carried out within the framework of the density functional theory (DFT) in the self-consistent formulation of Kohn and Sham.[17] This theory has proven to be particularly powerful for studying large electron systems in the presence of correlation.[18,19] According to Hohenberg and Kohn[20] and its generalization by Levy,[21] the exact ground-state energy of a many-body system is a unique functional of the electron density $n(\mathbf{r})$. DFT was initially developed in a spin-independent formalism. Later, effects of spin polarization were incorporated into the so-called SDFT.[22] In this approach the total energy is a functional of the spin-up and spin-down densities $n_\sigma(\mathbf{r})$, where $\sigma=(+,-)$ labels the spin. Equivalently, the energy is a functional of the total density

[a]Electronic mail: josep.planelles@qfa.uji.es.

$n(\mathbf{r})=n_+(\mathbf{r})+n_-(\mathbf{r})$ and spin-polarization $\zeta(\mathbf{r})=[n_+(\mathbf{r})-n_-(\mathbf{r})]/n(\mathbf{r})$. The ground state is found by minimizing the energy functional, leading to the well-known Kohn–Sham equations. Although the original proof of Hohenberg and Kohn[20] applies only to the ground state, it can be generalized to a large class of excited states, namely the energetically lowest state of each symmetry.[23] For example, it can be applied to the lowest state of a spherical QD with specific quantum numbers L, S, M, and M_S of the total orbital and spin angular momenta. This allows us, in particular, to study several low-lying electronic configurations with different M_S and to draw the spin phase diagram of the ground state of a semiconductor spherical quantum dot populated with different numbers of electrons versus a given control parameter.[24]

Since the calculations in this paper concern spherical QDs embedded in media with different dielectric constants and, additionally, carriers have different effective masses in the QD and the surrounding environment, we have to extend the SDFT to include variable effective mass and dielectric constants. We have recently carried out this extension and built the corresponding code. A fully detailed description of it can be found in Ref. 11. In short, it is an extension of the SDFT,[22] which includes (1) position-dependent effective mass by replacing the standard kinetic energy operator $-(\hbar^2/2m^*)\nabla^2$ by $-(\hbar^2/2)\nabla[(1/m^*)\nabla]$, corresponding to the case of variable effective mass. (2) Polarization of the Coulomb interaction arising from the dielectric mismatch, by numerically integrating the Poisson equation $\nabla[\varepsilon(r)\nabla\Psi(r)]=-4\pi n(r)$. (3) Self-energy, also coming from the dielectric mismatch, by incorporating the monoelectronic self-polarization potential according to the equations reported in Ref. 25. This dielectric confinement and the spatial confinement potentials are the genuine single-particle components of the Kohn–Sham potential. (4) The effect of dielectric mismatch on exchange by means of an appropriate scaling of the exchange functional, which is consistent with the Coulomb functional employed. And finally, (5) the correlation functional is also modified to incorporate the position-dependent parameters properly by means of a consistent scaling of Perdew–Zunger analytical functional that was employed.[26]

By using this code, we have thus drawn the ground state spin phase diagrams versus the QD radius R and the dielectric constant ε_{ext} of the surrounding medium. We have performed the calculations in the case of ZnS QD populated with $N=3$, 4, and 9 electrons, although, as discussed later, the qualitative trends obtained can be generalized to other materials and different numbers of electrons. The material parameters employed in our calculations, namely the electron effective mass $m^*_{\text{ZnS}}=0.34$ and dielectric constant $\varepsilon_{\text{ZnS}}=5.7$, are taken from Ref. 27. Spherical QDs are often prepared in water solutions ($\varepsilon_{H_2O}=1.78$) and polymeric media (dielectric constants ranging from $\varepsilon=2$ up to $\varepsilon=25$ have been reported for these media[28,29]). Thus, in our calculations, the external dielectric constant ε_{ext} of the surrounding medium ranges from $\varepsilon_{\text{ext}}=1$, corresponding to air or a vacuum, up to $\varepsilon_{\text{ext}}=50$. We assume an external effective mass $m^*_{\text{ext}}=1$ and a 4 eV confining potential barrier height.[30]

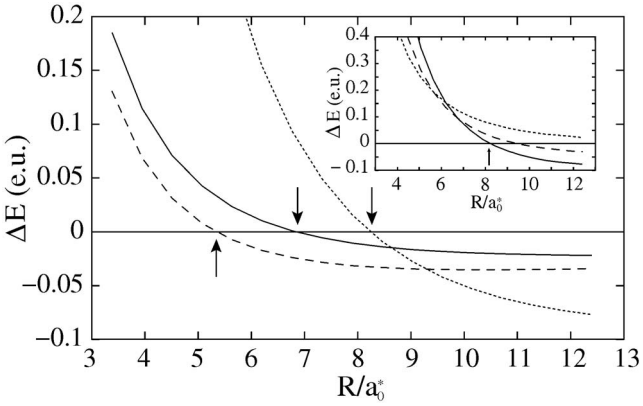

FIG. 1. Energy difference ΔE (e.u.) between spin polarized minus spin least-polarized electronic configurations vs QD radius R (e.u.) corresponding to a QD populated with three (full line), four (dashed line), and nine (dotted line) excess electrons. Arrows indicate the transition phase. Inset: Energy difference ΔE (e.u.) between the electronic configuration $1s1p^31d^5$ (full line), $1s^21p^31d^4$ (dashed line), and $1s1p^61d^2$ (dotted line) minus $1s^21p^61d$ vs QD radius R (e.u.). The arrow indicates the transition phase.

III. RESULTS AND DISCUSSION

The electronic configuration of an atom or a QD is determined by the balance of two factors, namely, the energy difference between consecutive orbitals and the pairing energy. In general, the Aufbau principle of sequential filling and the Hund rule of largest spin multiplicity in a shell are followed. However, as pointed out earlier, QDs can be tailored with precise properties, such as their radius. This fact allows the spin filling to be manipulated by tuning the energy gap between consecutive orbital levels.

We therefore start our study by exploring the critical radius leading to a change in the electronic configuration. In a first set of calculations we consider the same effective mass and dielectric constant for the QD and the surrounding medium. This allows us to work in effective atomic units and thus yield universal results. The only parameter included in these calculations is the height of the confining barrier, which is fixed to a value as large as 14 e.u. (effective Hartree). 14 e.u. corresponds to 4 eV for ZnS. We carry out calculations for a range of radii from 3 up to 12 effective Bohr radius a_0^* and a number of electrons $N=3$, 4, and 9. The results thus obtained are summarized in Fig. 1, where the energy difference ΔE (e.u.) between fully spin-polarized minus least spin-polarized configurations is plotted versus the QD radius R/a_0^*.

In all the cases that were studied, only two configurations, namely least-polarized and fully polarized, become the ground state. Thus, for $N=3$ the configuration $1s^21p$ is the lowest lying for $R<7a_0^*$ and $1s1p^2$ otherwise. For $N=4$ it is $1s^21p^2$ up to $R\sim5.5a_0^*$ and then $1s1p^3$. Finally, when $N=9$, $1s^21p^61d$ is the ground state if $R<8.3a_0^*$ and $1s1p^31d^5$ if R is larger.

One may wonder whether configurations others than least-polarized and fully polarized can lie the lowest. However, this does not hold for the cases that were studied. In order to show this in the most challenging case of $N=9$ electrons, in the inset in Fig. 1 we plot the difference ΔE between the energy of configurations $1s1p^31d^5$, $1s^21p^31d^4$, and

$1s1p^61d^2$, on the one hand, and $1s^21p^61d$, on the other, versus the QD radius. It can be seen that, for short effective radii, the larger the polarization is, the greater the resulting energy will be, while the opposite holds for large radii. There is, however, a central region where the energy ordering of configurations is neither one nor the other. Nevertheless, it can also be seen that only the spin least-polarized $1s^21p^61d$ and the fully spin-polarized $1s1p^31d^5$ configurations become the ground state.

Finally, since Fig. 1 is drawn in effective units, it is straightforward to conclude that QDs built of materials with small Bohr radii are the best candidates to be used for dielectric control of spin because the transition between configurations occurs at shorter radii and the energetic change resulting from QD manipulation is larger. In order to show the dielectric control of spin we chose QDs built of ZnS. It is a wide-gap semiconductor material, so that the conduction-valence coupling is negligible, i.e., nonparabolicity corrections can be safely neglected. This material has an effective Bohr radius of $a_0^* \sim 17a_0$ and an effective energy (1 e.u.) of $\sim 10^{-2}$ a.u. We then consider, first, the case of $N=3$ excess electrons and proceed as follows. From Fig. 1 we can see that the transition between configurations occurs at about $7a_0^*$, i.e., ~6 nm for ZnS. Thus, working within the range of radii between 4 and 8 nm, we calculate the energy of the relevant configurations of $N=3$ excess electrons ZnS QD embedded in media with a dielectric constant ranging from 1 up to 50. From these calculations we determine the ground state configuration for each pair $(R, \varepsilon_{\text{ext}})$. From this the phase diagram shown in Fig. 2(a) can be drawn. The line in this figure corresponds to the phase transition. Above the line the spin-polarized $1s1p^2$ configuration is the lowest lying, i.e., the ground state, while below it the ground state corresponds to the least-polarized $1s^21p$ configuration.

The physical source of dielectric control is polarization coming from the dielectric mismatch between the QD and the surroundings. In order to show this, we select the critical QD radius corresponding to the degeneracy of the two configurations when the QD is buried in a medium without dielectric mismatch ($\varepsilon_{\text{ext}}=\varepsilon_{\text{QD}}$). We then replace the external medium by another with a lower dielectric constant ($\varepsilon_{\text{ext}} < \varepsilon_{\text{QD}}$). The resulting dielectric mismatch leads each electron in the QD to induce a negative polarized charge at the QD border, thus enhancing the Coulomb interaction between carriers. This means that pairing energy is also enhanced and therefore the polarized configuration is preferred. In a similar way, the situation $\varepsilon_{\text{ext}} > \varepsilon_{\text{QD}}$ leads to a decrease in the Coulomb interaction and consequently to a decrease in the pairing energy so that a transition toward least-polarized configurations now occurs. This can be shown in Fig. 2(a) by choosing any point on the transition line and then moving left (toward smaller dielectric constants). By so doing we find the fully spin-polarized configuration. Nevertheless, moving right, and thus increasing ε_{ext}, we find the other least-polarized configuration.

The inset in Fig. 2(a) corresponds to a 5.5 nm radius ZnS QD. In this inset we have drawn the energy difference (meV) between the spin least- and fully polarized configuration versus ε_{ext}. This plot allows us to see, for example, that a "dry"

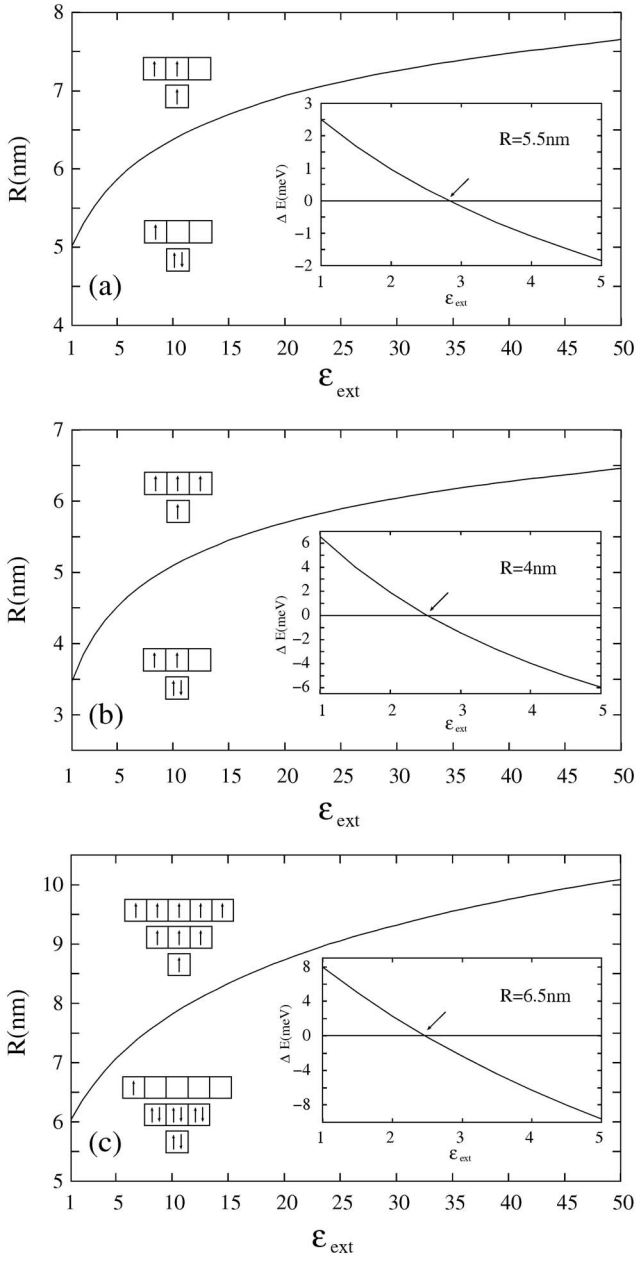

FIG. 2. Ground state phase diagram of a ZnS QD populated with three (a), four (b), and nine (c) excess electrons. Schematic diagrams for electronic configurations label the regions of existence (below/above the transition line) in the QD radius R (nm) vs the external dielectric constant ε_{ext} phase diagram. Insets: Energy difference ΔE (meV) of the spin least-polarized minus spin full polarized configuration vs the external dielectric constant ε_{ext} for a fixed value of the QD radius R (indicated at the top right of the inset). The arrow indicates the transition phase.

5.5 nm radius ZnS QD, i.e., this QD in air ($\varepsilon_{\text{ext}}=1$), has a fully polarized ground state configuration ($S=3/2$). However, if this QD is embedded in a polymeric solution of dielectric response, for example, $\varepsilon_{\text{ext}}=4$, a transition toward the least-polarized ($S=1/2$) configuration occurs. A solution with a dielectric constant of about 2.8 is able to tune degeneracy between both lowest-lying electronic configurations.

Figures 2(b) and 2(c) display the phase diagrams corresponding to $N=4$ and $N=9$ excess electrons. The results and diagrams obtained are qualitatively the same as in the case of $N=3$ electrons, but the changes in spin and/or energy are

larger. In the case $N=4$, the configurations involved have spins $S=1$ and $S=2$, while for $N=9$ a change in the dielectric environment can yield a transition between $S=1/2$ and $S=9/2$.

IV. CONCLUDING REMARKS

This paper is devoted to studying the role of dielectric mismatch in QD spin transitions. To this end, spin phase diagrams of QDs populated with different numbers of electrons versus the dielectric constant of the QD surroundings have been calculated. Our results show that it is possible to switch between high/low spin configurations by means of an appropriate QD environment and suggest the use of QD spin as a sensor of the dielectric response of a given medium.

ACKNOWLEDGMENTS

Financial support from UJI-Bancaixa Project No. P1-1B2006-03 (Spain) is gratefully acknowledged. Generalitat Valenciana FPI (M.R.) grant is also acknowledged.

[1]G. A. Prinz, Science **282**, 1660 (1998).
[2]S. Tarucha, D. G. Austing, T. Honda, R. J. van der Hage, and L. P. Kouwenhoven, Phys. Rev. Lett. **77**, 3613 (1996).
[3]*Semiconductor Spintronics and Quantum Computation*, edited by D. D. Awschalom, D. Loss, and N. Samarth (Springer, Berlin, 2002); Y. Masumoto and T. Takagahara, *Semiconductor Quantum Dots* (Springer, Berlin, 2002); A. D. Yoffe, Adv. Phys. **50**, 1 (2001); L. Jacak, P. Hawrylak, and A. Wójs, *Quantum Dots* (Springer, Berlin, 1998); T. Chakraborty, *Quantum Dots* (Elsevier, Amsterdam, 1999).
[4]C. Wang, M. Shim, and P. Guyot-Sionnest, Science **291**, 2390 (2001).
[5]S. Coe, W.-K. Woo, M. Bawendi, and V. Bulović, Nature (London) **420**, 800 (2002).
[6]W. U. Huynh, J. J. Dittmer, and A. P. Alivisatos, Science **295**, 2425 (2002).
[7]J. M. Klostranec and W. C. W. Chan, Adv. Mater. **18**, 1953 (2006).
[8]J. L. Movilla and J. Planelles, Phys. Rev. B **71**, 075319 (2005); J. L. Movilla, J. Planelles, and W. Jaskólski, *ibid.* **73**, 035305 (2006); J. Planelles and J. L. Movilla, *ibid.* **73**, 235350 (2006); J. L. Movilla and J. Planelles, *ibid.* **74**, 125322 (2006); F. Rajadell, J. L. Movilla, M. Royo, and J. Planelles, *ibid.* **76**, 115312 (2007).
[9]A. Orlandi, M. Rontani, G. Goldoni, F. Manghi, and E. Molinari, Phys. Rev. B **63**, 045310 (2001); A. Orlandi, G. Goldoni, F. Manghi, and E. Molinari, Semicond. Sci. Technol. **17**, 1302 (2002).
[10]A. Franceschetti and A. Zunger, Phys. Rev. B **62**, 2614 (2000).
[11]M. Pi, M. Royo, and J. Planelles, J. Appl. Phys. **100**, 073712 (2006).
[12]M. Royo, J. Planelles, and M. Pi, Phys. Rev. B **75**, 033302 (2007); J. Appl. Phys. **102**, 094304 (2007).
[13]S. Tarucha, D. G. Austing, Y. Tokura, W. G. van der Wiel, and L. P. Kouwenhoven, Phys. Rev. Lett. **84**, 2485 (2000).
[14]S. Sasaki, S. De Franceschi, J. M. Elzerman, W. G. van der Wiel, M. Eto, S. Tarucha, and L. P. Kouwenhoven, Nature (London) **405**, 764 (2000).
[15]M.-H. Chung, Phys. Rev. B **70**, 113302 (2004).
[16]L. Kouwenhoven and L. Glazman, Phys. World **14**, 33 (2001).
[17]W. Kohn and L. J. Sham, Phys. Rev. **140**, A1133 (1965).
[18]R. G. Parr and W. Yang, *Density-Functional Theory of Atoms and Molecules* (Oxford University Press, Oxford, 1989).
[19]E. Lipparini, *Modern Many-Particle Physics* (World Scientific, Singapore, 2003).
[20]P. Hohenberg and W. Kohn, Phys. Rev. **136**, B864 (1964).
[21]M. Levy, Proc. Natl. Acad. Sci. U.S.A. **76**, 6062 (1979).
[22]U. von Barth and L. Hedin, J. Phys. C **5**, 1629 (1972).
[23]O. Gunnarsson and B. I. Lundqvist, Phys. Rev. B **13**, 4274 (1976).
[24]Please note that, as in the case of unrestricted Hartree–Fock, SDFT wave functions are M_S but not S adapted.
[25]J. L. Movilla and J. Planelles, Comput. Phys. Commun. **170**, 144 (2005).
[26]J. P. Perdew and A. Zunger, Phys. Rev. B **23**, 5048 (1981).
[27]D. Dorfs, H. Henschel, J. Kolny, and A. Eychmüller, J. Phys. Chem. B **108**, 1578 (2004).
[28]A. Issac, Ch. von Borczyskowski, and F. Cichos, Phys. Rev. B **71**, 161302(R) (2005).
[29]J. Lee, B. Yang, R. Li, T. A. P. Seery, and F. Papadimitrakopoulos, J. Phys. Chem. B **111**, 81 (2007).
[30]The height for the spatial confining barrier of a QD in a vacuum should be set to the QD electroaffinity and, for a QD embedded in a given medium, to the corresponding band offset. In our calculation this height is always very large, and we deal with the ground state. Then, as the numerical results are insensitive to relatively small changes in the height of this very high spatial confining barrier, we have always assumed the same 4 eV height.